PHYSICAL REVIEW B VOLUME 51, NUMBER 7 15 FEBRUARY 1995-I

Semiclassical density-of-states and optical-absorption analysis of amorphous semiconductors

Stephen K. O'Leary* and Stefan Zukotynski
Department of Electrical and Computer Engineering, University of Toronto, Toronto, Ontario, Canada M5S 1A4

John M. Perz
Department of Physics and Scarborough College, University of Toronto, Toronto, Ontario, Canada M5S 1A7
(Received 9 March 1994; revised manuscript received 14 September 1994)

A semiclassical analysis of amorphous semiconductors is presented. This analysis, cast within an effective-mass setting, provides for the overall density-of-states by averaging a local density-of-states over a distribution of potential fluctuations. Our density-of-states results span the transition from the tail states to the band states, and both analytical and numerical results are obtained. We then determine the functional form of the optical-absorption coefficient, and show that both subgap and Tauc absorption edges are captured within this analytical framework. Finally, we apply this formalism to the case of hydrogenated amorphous silicon, and find that our results are consistent with those of experiment.

I. INTRODUCTION

In recent years, the fundamental properties of amorphous semiconductors have been the focus of considerable study. While much has been done, there are still many aspects of these semiconductors which are not fully understood. In particular, there are questions regarding how the disorder influences the electronic structure,[1] and there is the issue of what impact impurities, such as hydrogen in amorphous silicon, have upon the electronic and structural properties of these materials.[2] In order to resolve these issues, it is helpful to model these semiconductors.

From a theoretical perspective, the distribution of electronic states is one of the properties of fundamental interest in the study of amorphous semiconductors. While the distribution of states in a defect-free crystalline semiconductor ends abruptly at the band edge, in an amorphous semiconductor a tail of states encroaches upon the energy gap.[1] Analysis shows that many of the tail states are localized by the site disorder, and that there exists a critical energy, termed the mobility edge, which separates the localized states from their extended counterparts.[3,4] The localized states are responsible for many of the unique properties exhibited by amorphous semiconductors.

In order to study the general properties of amorphous semiconductors, it is convenient to adopt a continuum representation, in which the details of the local atomicity are ignored. For the case of amorphous semiconductors, for states in the vicinity of the mobility edge, the effective-mass approximation provides a convenient basis for analysis; see Grein and John.[5] In this approximation, the electronic structure is characterized by a pair of macroscopic one-electron potential profiles $V_c(\mathbf{R})$ and $V_v(\mathbf{R})$ corresponding to the behavior of charge carriers in the conduction and valence bands, respectively. Spatial variations in these potential profiles are to be expected, these variations reflecting the underlying structural disorder. By solving the wave equation for the spectrum of allowed one-electron states, the distribution of states may be determined.

Most effective-mass analyses of the distribution of localized tail states treat the bands as being comprised of an ensemble of randomly distributed independent potential wells, e.g., John *et al.*[6], Chan, Louie, and Phillips[7] and Bacalis, Economou, and Cohen.[8] By determining the binding energy corresponding to each potential well, and averaging over the distribution of such wells, the corresponding distribution of tail states may be determined. Within this context, the distribution of states is dictated by two factors: (1) the distribution of potential wells, and (2) the relationship between the binding energy of these wells and the well dimensions.

While potential-well models adequately characterize the distribution of localized tail states, they do not permit the evaluation of the distribution of states beyond the mobility edge. This is unfortunate, as many physical properties are influenced by states beyond this edge. In a recent review article, Cody[9] noted that there is currently no first-principles model which is able to account for both the distribution of tail states trapped in the site disorder, and the distribution of band states. However, we note that the semiclassical effective-mass approach of Kane,[10] originally developed to treat heavily doped crystalline semiconductors, captures both a distribution of tail states and a distribution of band states.

In this paper, we examine the electronic properties of amorphous semiconductors following the semi-classical approach of Kane.[10] In Sec. II we lay down the basic framework in which our analysis will proceed, focusing on the determination of the one-electron density-of-states (DOS) function $N(E)$, $N(E)\Delta E$ representing the number of one-electron states, per unit volume, between energies $[E, E+\Delta E]$. Then, in Sec. III, we use these DOS results to determine the functional properties of the optical-absorption coefficient $\alpha(\hbar\omega)$, these being of considerable theoretical and experimental interest.[11] This formalism is applied to the case of hydrogenated amorphous silicon (*a*-Si:H) in Sec. IV. Finally, conclusions are presented in Sec. V.

0163-1829/95/51(7)/4143(7)/$06.00

II. ANALYTICAL FRAMEWORK

The band tailing which occurs in amorphous semiconductors is fundamentally related to the disorder which characterizes these materials. There are many sources of disorder within an amorphous semiconductor, e.g., lattice vibrations, impurities, dangling bonds, weakened bonds, vacancies, and others.[12] Within the framework of the effective-mass approach, this disorder leads to fluctuations in the potential profiles $V_c(\mathbf{R})$ and $V_c(\mathbf{R})$. The dominant potential fluctuations are usually on the scale of a few lattice constants in range.

Focusing on the conduction band, Ziman[13] shows that if the kinetic energy of localization associated with the site disorder is small with respect to the magnitude of the conduction band potential fluctuations, then the semiclassical approach of Kane[10] is valid, i.e., the conduction-band DOS function $N_c(E)$ in a local region about $\mathbf{R}$ may be approximated as

$$N_c(E)=\begin{cases}\dfrac{\sqrt{2}m_c^{*3/2}}{\pi^2\hbar^3}\sqrt{E-V_c(\mathbf{R})}\ , & E\geq V_c(\mathbf{R})\\ 0\ , & E<V_c(\mathbf{R})\ ,\end{cases} \tag{1}$$

where m_c^* represents the effective mass of electrons in the conduction band, this being the standard DOS result for a three-dimensional continuum of states. To simplify our analysis, we treat $V_c(\mathbf{R})$ as a homogeneous, static, random field. To determine the overall DOS, we assert the ergodic hypothesis, and statistically average this local DOS over the distribution of conduction-band potential fluctuations, i.e.,

$$N_c(E)=\frac{\sqrt{2}m_c^{*3/2}}{\pi^2\hbar^3}\int_{-\infty}^{E}\sqrt{E-z}\,f_{V_c}(z)dz\ , \tag{2}$$

where $f_{V_c}(z)\Delta z$ denotes the probability that $V_c(\mathbf{R})$ is between $[z,z+\Delta z]$. Thus our calculation of the overall conduction-band DOS function reduces to an integration over this potential fluctuation distribution function $f_{V_c}(z)$.

We perform our subsequent analysis under the assumption of a Gaussian distribution of conduction-band potential fluctuations, i.e.,

$$f_{V_c}(z)=\frac{1}{\sqrt{2\pi\sigma_c^2}}\exp\left[-\frac{(z-\eta_c)^2}{2\sigma_c^2}\right]\ , \tag{3}$$

where η_c denotes the mean conduction-band potential level, σ_c being the corresponding standard deviation; see the Appendix for a determination of $f_{V_c}(z)$ from first principles. From Eqs. (2) and (3), it can be shown that the overall conduction-band DOS function

$$N_c(E)=\frac{\sqrt{2\sigma_c}m_c^{*3/2}}{\pi^2\hbar^3}\Xi\left[\frac{E-\eta_c}{\sigma_c}\right]\ , \tag{4}$$

where the dimensionless DOS function $\Xi(z)$ is defined as

$$\Xi(z)\equiv\frac{1}{\sqrt{2\pi}}\int_{-\infty}^{z}\sqrt{z-x}\exp\left[-\frac{x^2}{2}\right]dx\ . \tag{5}$$

This result suggests that while η_c determines the positioning of this DOS function, σ_c dictates the spread.

The dimensionless DOS function $\Xi(z)$ is displayed in Figs. 1(a) and 1(b). Note that these plots exhibit the basic features expected of the amorphous semiconductor DOS function.[1] We find that as $z\rightarrow\infty$

$$\Xi(z)\rightarrow\sqrt{z}\ , \tag{6}$$

while as $z\rightarrow-\infty$

$$\Xi(z)\rightarrow\frac{1}{2\sqrt{2}}(-z)^{-3/2}\exp\left[-\frac{z^2}{2}\right]\ . \tag{7}$$

Thus high in the band,

$$N_c(E)\rightarrow\frac{\sqrt{2}m_c^{*3/2}}{\pi^2\hbar^3}\sqrt{E-\eta_c}\ , \tag{8}$$

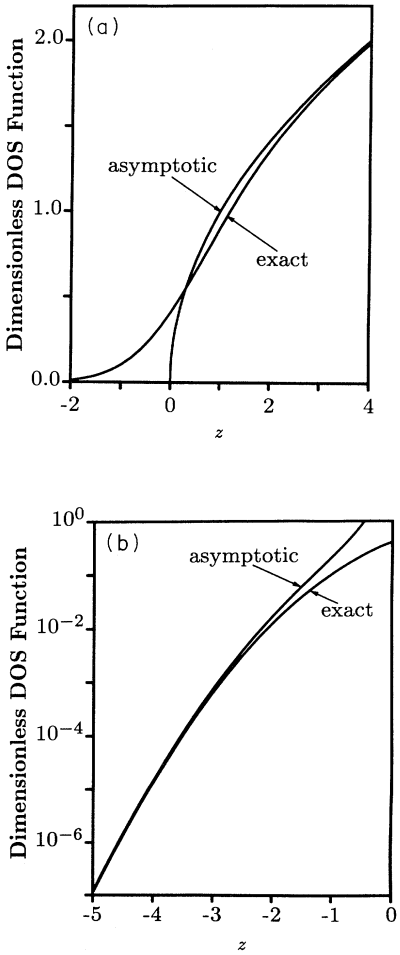

FIG. 1. (a) The dimensionless DOS function $\Xi(z)$ (linear scale). The asymptotic form Eq. (6) is also depicted. (b) The dimensionless DOS function $\Xi(z)$ (logarithmic scale). The asymptotic form Eq. (7) is also depicted.

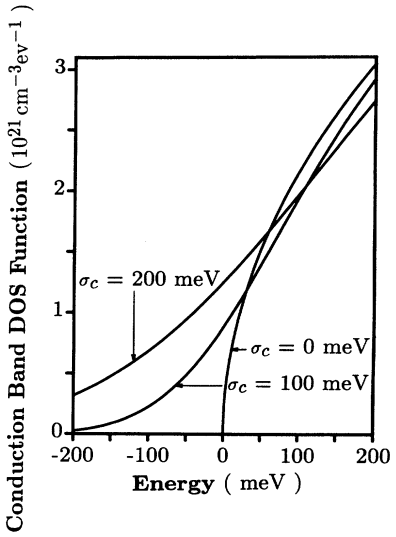

FIG. 2. The conduction-band DOS function $N_c(E)$, corresponding to various selections of σ_c (linear scale). The conduction-band mean potential level η_c is set equal to zero in all cases.

while deep in the tail,

$$N_c(E)\sim\exp\left[-\frac{|E-\eta_c|^2}{2\sigma_c^2}\right] . \tag{9}$$

Ziman,[13] using semiclassical transport arguments, suggests that the mobility edge occurs at energy $\eta_c-\sigma_c$.

To study the effect of disorder, we examine the sensitivity of $N_c(E)$ to variations in σ_c. In Fig. 2, we plot this DOS function for a number of selections of σ_c, m_c^* being set to the free-electron mass m_e. In the disorderless limit, where $\sigma_c\rightarrow 0$,

$$N_c(E)\rightarrow\begin{cases}\dfrac{\sqrt{2}m_c^{*3/2}}{\pi^2\hbar^3}\sqrt{E}-\eta_c\ , & E\geq\eta_c\\ 0\ , & E<\eta_c\ .\end{cases} \tag{10}$$

For finite σ_c, a distribution of tail states appears. As σ_c increases from this disorderless limit, the tail further encroaches into the gap. It may be shown formally that the total number of states remains conserved, regardless of the strength of the disorder. Thus we conclude that the potential fluctuations are redistributing states, removing them from the band and adding them to the tail.

A similar valence-band analysis can be performed. Assuming that the valence band kinetic energy of localization associated with the site disorder is small relative to the magnitude of the valence-band potential fluctuations, and assuming a Gaussian distribution of valence-band potential fluctuations, the overall valence-band DOS function $N_v(E)$ may be shown to be equal to

$$N_v(E)=\frac{\sqrt{2\sigma_v}m_v^{*3/2}}{\pi^2\hbar^3}\Xi\left[\frac{\eta_v-E}{\sigma_v}\right] , \tag{11}$$

where η_v denotes the mean valence-band potential level, σ_v being the corresponding standard deviation.

We now quantify the Ziman condition. For potential fluctuations of linear range L the kinetic energy of localization associated with the site disorder is of the order of

$$\Delta=\frac{\hbar^2}{2m^*L^2} . \tag{12}$$

Under the assumption of a Gaussian distribution of potential fluctuations, the Ziman condition is satisfied if

$$\sigma\gg\Delta . \tag{13}$$

If the kinetic energy of localization associated with the site disorder is large, and the Ziman condition is not exactly satisfied, Ziman[13] suggests that the semiclassical formalism of Kane may be modified by a simple energy shift by the zero point energy. This will merely shift the results without changing their fundamental form.

III. OPTICAL ABSORPTION IN AMORPHOUS SEMICONDUCTORS

In an amorphous semiconductor, momentum is a poor quantum number. As a result, only energy conservation need be satisfied for a successful optical transition. This being the case, an elementary analysis shows that the optical-absorption coefficient $\alpha(\hbar\omega)$ may be expressed as

$$\alpha(\hbar\omega)\simeq D^2(\hbar\omega)J(\hbar\omega) , \tag{14}$$

where $J(\hbar\omega)$ denotes the joint density of states, $D(\hbar\omega)$ being the optical transition matrix element.[14–17] At low temperatures, in the undoped or lightly doped case, this joint density-of-states function may be approximated as

$$J(\hbar\omega)\simeq\int_{-\infty}^{\infty}N_c(E)N_v(E-\hbar\omega)dE . \tag{15}$$

Thus, from Eqs. (4), (11), (14), and (15), we see that

$$\alpha(\hbar\omega)\simeq D^2(\hbar\omega)\frac{\sqrt{2}m_c^{*3/2}}{\pi^2\hbar^3}\frac{\sqrt{2}m_v^{*3/2}}{\pi^2\hbar^3}\times\mathscr{J}(\hbar\omega;\eta_c,\eta_v,\sigma_c,\sigma_v) , \tag{16}$$

where $\mathscr{J}(\hbar\omega;\eta_c,\eta_v,\sigma_c,\sigma_v)$ denotes the normalized joint density-of-states function, this being defined as follows:

$$\mathscr{J}(\hbar\omega;\eta_c,\eta_v,\sigma_c,\sigma_v)\equiv\sqrt{\sigma_c}\sqrt{\sigma_v}\int_{-\infty}^{\infty}\Xi\left[\frac{E-\eta_c}{\sigma_c}\right]\Xi\left[\frac{\eta_v+\hbar\omega-E}{\sigma_v}\right]dE . \tag{17}$$

Following the lead of Grein and John,[18] we assume that $D(\hbar\omega)$ exhibits a relatively weak dependence on $\hbar\omega$, and focus our analysis on determining the functional properties of $\mathscr{J}(\hbar\omega;\eta_c,\eta_v,\sigma_c,\sigma_v)$.

We first consider the form of $\mathscr{J}(\hbar\omega;\eta_c,\eta_v,\sigma_c,\sigma_v)$ in the disorderless limit, i.e., as $\sigma_c\rightarrow 0$ and $\sigma_v\rightarrow 0$. From Eq. (17), we see that in this limit

$$\mathcal{J}(\hbar\omega;\eta_c,\eta_v,\sigma_c,\sigma_v)\rightarrow\begin{cases}\frac{\pi}{8}(\hbar\omega-E_{g_0})^2\ , & \hbar\omega\geq E_{g_0}\\ 0\ , & \hbar\omega<E_{g_0}\end{cases} \tag{18}$$

where

$$E_{g_0}=\eta_c-\eta_v\ . \tag{19}$$

This parabolic absorption edge, arising as a consequence of optical transitions between the bands, is referred to as the Tauc absorption edge,[9,19] E_{g_0} being the value of the Tauc gap in the disorderless limit.

We now introduce the effect of disorder. In Fig. 3(a), we plot $\sqrt{\mathcal{J}(\hbar\omega;\eta_c,\eta_v,\sigma_c,\sigma_v)}$ for a number of selections of σ_c and σ_v, E_{g_0} being held at 2.0 eV; $\mathcal{J}(\hbar\omega;\eta_c,\eta_v,\sigma_c,\sigma_v)$ may be shown formally to be only a function of $\hbar\omega-E_{g_0}$, σ_c, and σ_v. It is seen that for high energies in all cases, $\sqrt{\mathcal{J}(\hbar\omega;\eta_c,\eta_c,\sigma_c,\sigma_v)}$ approaches a linear functional dependence on $\hbar\omega$, i.e., Tauc absorption edges are observed. Extrapolating this high-energy Tauc absorption behavior to low energies, an extrapolated Tauc gap may be defined; see, for example, Kruzelecky *et al.*[19] It is seen that the extrapolated Tauc gap E_g decreases monotonically from E_{g_0} as the disorder is increased. This result suggests that the disorder, in of itself, directly influences the extrapolated Tauc gap, as was found experimentally by Cody *et al.*[20]

In Fig. 3(b), we depict the functional dependence of these $\mathcal{J}(\hbar\omega;\eta_c,\eta_v,\sigma_c,\sigma_v)$ plots over a much broader range of photon energies. This time, however, we focus our analysis on the low-energy optical-absorption tail that is observed in the subgap region, this tail corresponding to optical transitions between the tail states. We note that the width of this tail decreases monotonically as the disorder decreases, as was observed experimentally by Cody *et al.*[20]

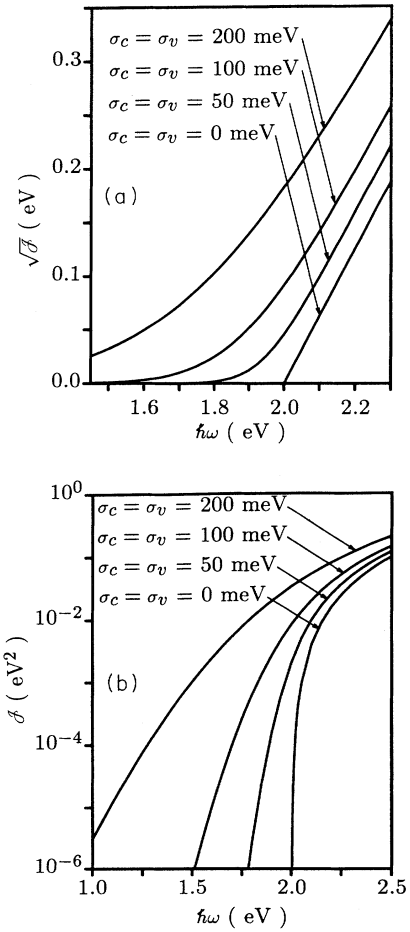

FIG. 3. (a) The square root of the normalized joint density of states function $\mathcal{J}(\hbar\omega;\eta_c,\eta_v,\sigma_c,\sigma_v)$ (linear scale). The disorderless Tauc gap E_{g_0} is set to 2 eV in all cases. (b) The normalized joint density of states function $\mathcal{J}(\hbar\omega;\eta_c,\eta_v,\sigma_c,\sigma_v)$ (logarithmic scale). The disorderless Tauc gap E_{g_0} is set to 2 eV in all cases.

IV. APPLICATION TO *a*-Si:H

We now demonstrate that our DOS results are consistent with those of experiment. At the outset, it must be pointed out that there are no direct means of determining, experimentally, the distribution of states. Furthermore, most means of determining the DOS are only valid over very limited ranges of energy. As a result, the exact form of the DOS function is still subject to debate, e.g., see Tiedje[21] and Longeaud and Vanderhaghen.[22]

In this analysis, we use DOS results which are derived from time-of-flight measurements of high-quality *a*-Si:H, these results being sensitive to the distribution of states just below the mobility edge. In Fig. 4, we display the

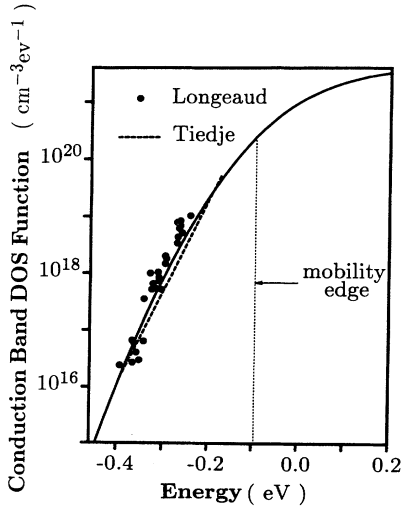

FIG. 4. The conduction-band DOS function $N_c(E)$. The results of Tiedje (Fig. 17 of Ref. 21) and Longeaud and Vanderhaghen (Fig. 5 of Ref. 22) are shown. Our theoretical result is represented by the solid line; $\sigma_c=94$ meV and $\eta_c=0$ meV. The mobility edge is represented by the light dotted line; this edge is at energy level $\eta_c-\sigma_c$, in accordance with Ziman's (Ref. 13) suggestion.

conduction-band DOS results of Tiedje[21] and the more recent results of Longeaud and Vanderhaghen;[22] the properties of these samples are believed to be quite similar. Tiedje[21] interpreted his results to necessarily yield a linear-exponential distribution of states, while the results of Longeaud and Vanderhaghen[22] were obtained in a more direct manner. Setting $m_c^* = 1.08 m_e$, this being the DOS effective mass associated with crystalline silicon,[23] we find that selections of σ_c between 90 and 100 meV yield distributions of states which are consistent with these experimental results. In Fig. 4, we plot the case of $\sigma_c = 94$ meV. A similar valence-band analysis, m_v^* being set equal to 0.56 m_e, shows that selections of σ_v between 130 and 145 meV leads to distributions of states which are consistent with the valence-band DOS experimental results of Tiedje.[21]

To assess the validity of our DOS fits over a much broader range of energy levels, we consider the form of the optical-absorption coefficient $\alpha(\hbar\omega)$, since $\alpha(\hbar\omega)$ depends on both the distributions of band states and tail states. In Fig. 5, we plot the optical-absorption data of Cody *et al.*[20] and Roxolo *et al.*;[24] the properties of these samples are believed to be quite similar to those of Tiedje[21] and Longeaud and Vanderhaghen.[22] These results have been scaled to facilitate a comparison with $\mathcal{J}(\hbar\omega;\eta_c,\eta_v,\sigma_c,\sigma_v)$, the scaling between $\alpha(\hbar\omega)$ and $\mathcal{J}(\hbar\omega;\eta_c,\eta_v,\sigma_c,\sigma_v)$ being consistent with that of Jackson *et al.*[16] Alongside, we plot our theoretical result for two different parameter selections: (1) $\sigma_c = 94$ meV, $\sigma_v = 140$ meV, and $E_{g_0} = 2$ eV, and (2) $\sigma_c = 94$ meV, $\sigma_v = 132$ meV, and $E_{g_0} = 2$ eV. Note that the selections of σ_c and σ_v are consistent with our previous analysis, i.e., Fig. 4. The

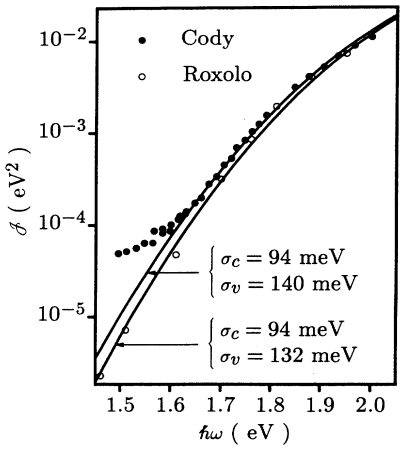

FIG. 5. Optical absorption: A comparison with experiment. The normalized joint density-of-states functions $\mathcal{J}(\hbar\omega;\eta_c,\eta_v,\sigma_c,\sigma_v)$, for two different parameter selections are represented by the solid lines. The disorderless Tauc gap E_{g_0} is set to 2 eV in all cases. The data points of Cody *et al.* (Fig. 1 of Ref. 20), for the case of room-temperature high-quality *a*-Si:H are depicted; these points correspond to the solid upper triangle data points of Cody *et al.* (Ref. 20). The data points of Roxolo *et al.* (Fig. 2 of Ref. 24) are also shown.

disorderless Tauc gap, E_{g_0} is set to 2 eV, this being the disorderless limit Tauc gap observed experimentally by Cody *et al.*[20] We note that our theoretical projections correspond well with experiment, the transition from the subgap absorption tail to the Tauc region being captured quite adequately by our semiclassical analysis, over many orders of magnitude. For values of $\hbar\omega$ less than 1.60 eV, a discrepancy between the results of theory and the experimental results of Cody *et al.*[20] is noted. This discrepancy may be attributed to a number of factors: (1) the existence of dangling bonds and other such impurities, (2) the breakdown in the effective-mass approximation as one goes deeper into the gap (see Grein and John[18]), and (3) the use of a direct optical measurement technique, which becomes poor at low values of $\alpha(\hbar\omega)$. Note that the more recent results of Roxolo *et al.*[24] agree with our theoretical predictions over a much broader range of photon energies.

Throughout our analysis, we have implicitly assumed that the Ziman condition is satisfied. We now test this assumption for the case of *a*-Si:H. Hydrogen atoms are believed to produce the dominant potential fluctuations in this material; see Brodsky[25] and O'Leary, Zukotynski, and Perz.[26] High-quality *a*-Si:H is characterized by concentrations of hydrogen of the order of 10 at. %. At such concentrations, the distance between the hydrogen-atom clusters is somewhere between 10 and 13 Å.[27,28] Thus, for the conduction band, Δ is somewhere between 18 and 35 meV. While this is not completely negligible compared to σ_c, it is a factor of 3–4 lower, and is thus small enough to suggest that potential fluctuations play the principal role in determining the DOS of *a*-Si:H. Corrections for the kinetic energy of localization, such as the energy shift suggested by Ziman, are needed to obtain more accurate results. The form of the DOS function, $N(E)$, and of the optical-absorption coefficient, $\alpha(\hbar\omega)$, will not be modified by such an energy shift.

V. CONCLUSIONS

In conclusion, we have presented a simple semiclassical analysis of amorphous semiconductors which successfully predicts some of the basic qualitative and quantitative DOS features. This analysis spans the transition from the tail states to the band states, and focuses on potential fluctuation effects. This contrasts with the potential-well approach in which the focus is the kinetic energy of localization, only the localized tail states being considered. Our results suggest that, for high-quality *a*-Si:H at least, potential fluctuations effects play the dominant role in shaping the distribution of states, the kinetic energy of localization playing a lesser role.

Using this analysis, we have demonstrated analytically that as the disorder increases from the disorderless limit, a tail of states emerges, these tail states being produced at the expense of band states. Corresponding to these tail states, a subgap absorption edge appears. We also observe a high-energy Tauc absorption edge, and note that the extrapolated Tauc gap E_g varies as a function of disorder, all other parameters being held fixed. This confirms the experimental results of Cody *et al.*,[20] and

provides insight into the fundamental relationship between the Tauc gap E_g and the characteristic width of the subgap absorption tail.

ACKNOWLEDGMENTS

The authors wish to thank C. Aversa, Dr. A. Pindor, and Professor S. John for interesting and helpful discussions.

APPENDIX: DISTRIBUTION DETERMINATION

Throughout our analysis, we have assumed a Gaussian distribution of potential fluctuations. This assumption is usually justified by means of the central limit theorem; see John *et al.*[6] However, more recent analyses have suggested that substantial deviations from this Gaussian distribution of potential fluctuations may arise, e.g., Kemp and Silver.[29] Clearly, such deviations may have a dramatic effect on the distribution of tail states, and should be investigated. Thus we present a point defect formalism which will allow one to determine $f_{V_c}(z)$ from first principles.

We assume that the physical structure of an amorphous semiconductor is characterized by a number of point defects, these point defects being distributed throughout an otherwise perfect solid.[13] These point defects represent the effect of the various forms of disorder. Each point defect will induce a certain conduction-band potential fluctuation, and the conduction-band potential $V_c(\mathbf{R})$ may be written as a sum over these potential fluctuations, i.e.,

$$V_c(\mathbf{R})=V_c'(\mathbf{R})+V_c^0 , \tag{A1}$$

where V_c^0 denotes the level of $V_c(\mathbf{R})$ which would result if there were no point defects, and

$$V_c'(\mathbf{R})=\sum_m v_c^m(\mathbf{R}-\mathbf{r}_m) , \tag{A2}$$

where $\mathbf{r}_m$ denotes the location of the mth point defect, $v_c^m(\cdot)$ being the conduction-band potential fluctuation associated with that particular point defect. Clearly the statistical properties of $V_c'(\mathbf{R})$ depend on (1) the distribution of these point defects, and (2) the form of the individual point defect potential profiles, $v_c^m(\cdot)$.

We treat the case of there being N types of point defect, these point defects being uniformly and independently distributed. It can be shown that the probability of finding n such type-i ($i=1,\ldots,N$) point defects in a volume V is

$$\text{Prob}[n \text{ type-}i \text{ point defects in } V]=e^{-\lambda^{(i)}V}\frac{(\lambda^{(i)}V)^n}{n!} , \tag{A3}$$

where $\lambda^{(i)}$ denotes the average number of type-i point defects per unit volume. If we associate with each type-i point defect a conduction-band potential fluctuation $v_c^{(i)}(\cdot)$, by applying either the method of Klauder,[10] or these of Holtsmark[30] and Chandrasekhar,[31] it can be shown, from Eq. (A3), that

$$f_{V_c'}(z)=\frac{1}{2\pi}\int_{-\infty}^{\infty}\exp\left[-i\omega z+\sum_{i=1}^{N}\lambda^{(i)}\int(e^{i\omega v_c^{(i)}(\mathbf{r})}-1)d\mathbf{r}\right]dw , \tag{A4}$$

where all integrals over $d\mathbf{r}$ are taken over three-dimensional space in its entirety. This result is a generalization of that from Kane;[10] Kane[10] only dealt with the $N=1$ case. A similar analysis may be performed in the valence band, the valence-band potential fluctuations being distinct from those in the conduction band.

Using the method of stationary phase, in the limit of infinite point defect density, a Gaussian distribution of potential fluctuations is found, i.e.,

$$f_{V_c}(z)=\frac{1}{\sqrt{2\pi\sigma_c^2}}\exp\left[-\frac{(z-\eta_c)^2}{2\sigma_c^2}\right] , \tag{A5}$$

where

$$\eta_c=\sum_{i=1}^{N}\lambda^{(i)}\int v_c^{(i)}(\mathbf{r})d\mathbf{r}+V_c^0 \tag{A6}$$

and

$$\sigma_c^2=\sum_{i=1}^{N}\lambda^{(i)}\int[v_c^{(i)}(\mathbf{r})]^2d\mathbf{r} . \tag{A7}$$

For finite point defect densities, deviations from this Gaussian distribution may occur, particularly for energies far from the mean, i.e., when $|(z-\eta_c)/\sigma_c|\gg 1$.

We now estimate the magnitude of σ_c from this point defect formalism. As was mentioned earlier, there are many sources of disorder within an amorphous semiconductor. From basic considerations, it is reasonable to assume that the density of point defects in an amorphous semiconductor is of the order of 10^{21} cm^{-3}. Furthermore, it is reasonable to assume that each potential fluctuation is of the order of a few lattice constants in range, and that the magnitude of these potential fluctuations is of the order of 100 meV; Brodsky[25] and O'Leary, Zukotynski, and Perz[26] suggest that the magnitude of the conduction-band potential fluctuations exhibited within *a*-Si:H are of the order of 100 meV. From Eq. (A7), it may then be shown that σ_c is of the order of 100 meV. This is consistent with the selections of σ_c that we have made. A similar analysis may be performed for σ_v.

*Electronic address: oleary@eecg.toronto.edu

[1] N. F. Mott and E. A. Davis, *Electronic Processes in Non-Crystalline Materials*, 2nd ed. (Clarendon, Oxford, 1979).

[2] A. Chenevas-Paule, in *Hydrogenated Amorphous Silicon*, Semiconductors and Semimetals Vol. 21, edited by J. I. Pankove (Academic, New York, 1984), Pt. A, p. 247.

[3] N. F. Mott, Adv. Phys. **16**, 49 (1967).

[4] N. F. Mott, Philos. Mag. **17**, 1259 (1968).

[5]C. H. Grein and S. John, Phys. Rev. B **36**, 7457 (1987).
[6]S. John, C. Soukoulis, M. H. Cohen, and E. N. Economou, Phys. Rev. Lett. **57**, 1777 (1986).
[7]C. T. Chan, S. G. Louie, and J. C. Phillips, Phys. Rev. B **35**, 2744 (1987).
[8]N. Bacalis, E. N. Economou, and M. H. Cohen, Phys. Rev. B **37**, 2714 (1988).
[9]G. D. Cody, J. Non-Cryst. Solids **141**, 3 (1992).
[10]E. O. Kane, Phys. Rev. **131**, 79 (1963).
[11]G. D. Cody, in *Hydrogenated Amorphous Silicon* (Ref. 2), Pt. B, p. 11.
[12]D. A. Papaconstantopoulos and E. N. Economou, Phys. Rev. B **24**, 7233 (1981).
[13]J. M. Ziman, *Models of Disorder* (Cambridge, New York, 1979).
[14]The optical transition matrix element $D(\hbar\omega)$ depends on many parameters. For a complete discussion, see Ref. 15, Jackson *et al.* (Ref. 16), and Street (Ref. 17).
[15]L. Ley, in *The Physics of Hydrogenated Amorphous Silicon II,* edited by J. D. Joannopoulos and G. Lucovsky, Topics in Applied Physics Vol. 56 (Springer-Verlag, New York, 1984), p. 61.
[16]W. B. Jackson, S. M. Kelso, C. C. Tsai, J. W. Allen, and S.-J. Oh, Phys. Rev. B **31**, 5187 (1985).
[17]R. A. Street, *Hydrogenated Amorphous Silicon* (Cambridge, New York, 1991).
[18]C. H. Grein and S. John, Phys. Rev. B **39**, 1140 (1989).
[19]R. V. Kruzelecky, D. Racansky, S. Zukotynski, and J. M. Perz, J. Non-Cryst. Solids **99**, 89 (1988).
[20]G. D. Cody, T. Tiedje, B. Abeles, B. Brooks, and Y. Goldstein, Phys. Rev. Lett. **47**, 1480 (1981).
[21]T. Tiedje, in *Hydrogenated Amorphous Silicon* (Ref. 2), Pt. C, p. 207.
[22]C. Longeaud and R. Vanderhaghen, Philos. Mag. **61**, 277 (1990).
[23]D. A. Neamen, *Semiconductor Physics and Devices* (Irwin, Boston, 1992).
[24]C. B. Roxolo, B. Abeles, C. R. Wronski, G. D. Cody, and T. Tiedje, Solid State Commun. **47**, 985 (1983).
[25]M. H. Brodsky, Solid State Commun. **36**, 55 (1980).
[26]S. K. O'Leary, S. Zukotynski, and J. M. Perz, J. Appl. Phys. **72**, 2272 (1992).
[27]Baum *et al.* (Ref. 28) suggest that hydrogen in *a*-Si:H appears in clusters, an average of six hydrogen atoms being associated with each cluster. Considering that roughly 4 at. % hydrogen is electronically neutral [see Baum *et al.* (Ref. 28) for details] it is reasonable to conclude that the distance between the cluster centers is between 10 and 13 Å.
[28]J. Baum, K. K. Gleason, A. Pines, A. N. Garroway, and J. A. Reimer, Phys. Rev. Lett. **56**, 1377 (1986).
[29]M. Kemp and M. Silver, Appl. Phys. Lett. **62**, 1487 (1993).
[30]J. Holtsmark, Ann. Phys. **58**, 577 (1919).
[31]S. Chandrasekhar, Rev. Mod. Phys. **15**, 1 (1943).